High-power high-brightness 2-μm continuous wave laser with a double-end diffusion-bonded Tm, Ho:YVO$_4$ crystal

Gang Li (李 纲)[1,2], **Yuqiu Gu (谷渝秋)**[2], **Baoquan Yao (姚宝权)**[1*], **Lianqiang Shan (单连强)**[2], **and Yuezhu Wang (王月珠)**[1]

[1]*National Key Laboratory of Tunable Laser Technology, Harbin Institute of Technology, Harbin 150001, China*

[2]*Science and Technology on Plasma Physics Laboratory, Research Center of Laser Fusion,*

China Academy of Engineering Physics, Mianyang 621900, China

*Corresponding author: yaobq08@hit.edu.cn

This letter demonstrates an efficient high-power high-brightness 2-μm continuous-wave (CW) laser with double-end, diffusion-bonded Tm, Ho:YVO$_4$ crystal cooled with liquid N$_2$. The reduction in thermal stress in the composite Tm, Ho:YVO$_4$ rod enabled the laser to achieve a laser output power of 23.4 W at 2.05 μm, which is 1.37 times higher than that of the non-composite Tm, Ho:YVO$_4$ rod. The corresponding slope efficiency is 37.3% and the optical–optical conversion efficiency is 35.4%. The beam quality M^2 factor is about 1.85 at 20 W output level with circularly symmetric beam spot.

OCIS codes: 140.3480, 140.3580, 140.5680.

doi: 10.3788/COL201311.091404.

Solid-state lasers that emit around 2-μm have wide applications in optical metrology, atmospheric sounding, free-space communication, medicine, and so on. In particular, high-power, high-brightness 2-μm lasers are efficient pump sources for 3–5 μm or 8–12 μm mid-/long-wave infrared ZnGeP$_2$ optical parametric oscillators (ZGP OPOs)[1−3]. The rare earth ions commonly used to obtain 2-μm laser radiation are Tm and Ho ions. Furthermore, the Tm-Ho co-doped laser media are persistently attractive because of its many remarkable properties, such as diode-pump availability, two-for-one pumping via cross relaxation, efficient energy transfer from Tm^{3+} to Ho^{3+}, large emission cross section of Ho^{3+}, and so on[4]. The cooperative up-conversion losses are significant in Tm-Ho codoped laser system[5]; however, the losses can be reduced under cryogenic temperatures to achieve high-power and high-brightness operation by increasing the complexity of the laser setup[6,7]. Moreover, the end-pumping scheme is developed to achieve high-brightness laser output because it has superior spectral and spatial pump beam overlap and resonator mode, compared with other pump configurations. However, efficient high-power high-brightness laser (TEM$_{00}$ mode) operation using the end-pumping scheme is seriously hindered by thermal effects, especially thermal fracture for those laser media with relatively low fracture stresses. For example, the fracture stress of YVO$_4$ crystal is only 53 MPa, which is nearly 2.6 times lower than that of YAG (138 MPa)[8]. Consequently, novel techniques such as double-end pumping, side pumping, and diffusion-bonded laser rod utilization have been developed to improve the thermal uniformity of the laser rod and to achieve high-power operation[9−11].

Recent experimental results have shown that Tm, Ho:YVO$_4$ crystal is an excellent laser material for 2-μm laser radiation, either for high-power (>10 W) or for mode-locking operation[12,13]. Up to 20 W of laser output has been obtained under liquid N$_2$-cooled temperature

using two non-composite Tm, Ho:YVO$_4$ rod connected in series in a laser resonator[7]. However, further power scaling of the Tm, Ho:YVO$_4$ laser via the end-pumping scheme is limited by crystal thermal fracture because of its relatively low fracture stresses, as previously pointed out. To simplify the experimental setup used by Yao *et al.*[7] without influencing the output power, we demonstrate an efficient high-power, high-brightness 2-μm laser with double-end, diffusion-bonded Tm, Ho:YVO$_4$ crystal. The composite laser rods would reduce the thermal stress, thereby lowering the risk of thermal fracture, as well as produce a weaker thermal lensing effect compared with non-composite laser rods, which is very beneficial for high-power scaling[11]. The resulting setup achieved a laser output power of 23.4 W at 2 μm, which is 1.37 times higher than the non-composite laser rod. The corresponding slope efficiency and optical-optical conversion efficiency were 37.3% and 35.4%, respectively. Furthermore, the beam quality M^2 factor was about 1.85 at 20 W output level.

The experimental setup for the composite Tm, Ho:YVO$_4$ laser is shown in Fig. 1. The 3 × 3 × 14 (mm) diffusion-bonded crystal, called YVO$_4$ Tm, Ho:YVO$_4$/YVO$_4$, with double 3-mm-long, undoped YVO$_4$ end bonded to both facets of 4 at.% Tm^{3+} and 0.4 at.% Ho^{3+} active Tm, Ho:YVO$_4$ crystal, was grown using the Czochralski method and an a-cut along the growth direction. The two end faces of the composite crystal were both anti-reflection (AR) coated at 795 nm ($R < 0.5\%$) and 2 μm ($R < 0.3\%$). The crystal was wrapped in indium foil and held in a copper heat sink connected with a small Dewar flask filled with 300 mL of liquid N$_2$. The laser diode (LD) pump is a fiber-coupled LD with a maximal output power of 70 W actual power = 66 W and an emission wavelength ranged from 789 to 794 nm, depending on heat sink temperature and pump current. The fiber diameter was 400 μm and the numerical aperture (NA) was 0.22. The pump beam was
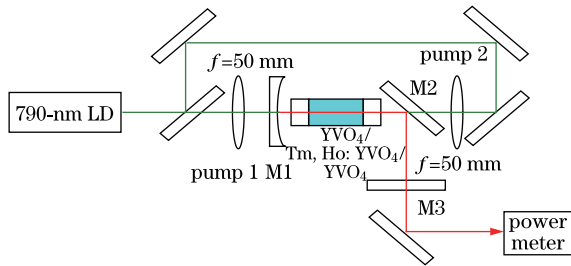
Fig. 1. Experimental setup of the composite Tm, Ho:YVO$_4$ laser.
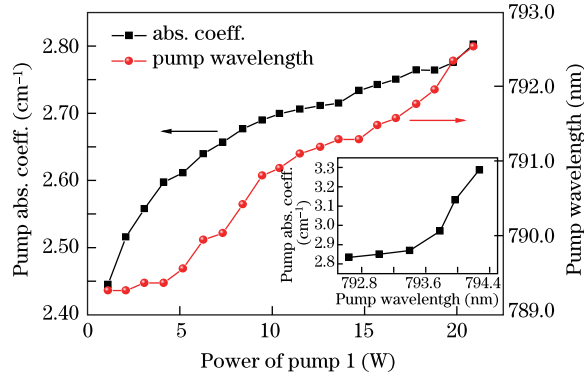
Fig. 2. Experimentally measured pump absorption coefficient under non-lasing conditions with the LD heat sink temperature maintained at 30 °C.

divided into two pump beams and focused to radius of about 400 μm inside the crystal for dual-end rod pumping. The simple L-shaped laser resonator had a physical length of about 105 mm. The input mirror M1 was a plano-concave mirror with curvature radius of 800 mm, which had a high transmission at the pump wavelength ($T > 95\%$) and high reflectivity at the laser wavelength ($R > 99.5\%$). M2 was a 45° dichroic mirror with reflectivity $> 99.5\%$ at the laser wavelength and transmission $>95\%$ at the pump wavelength. The output mirror M3 was flat with part of transmission at the laser wavelength. For comparison, a non-composite $3 \times 3 \times 8$ (mm) Tm, Ho:YVO$_4$ crystal, with the same doped concentrations as the composite one, was also investigated using the same experimental setup except the composite crystal was replaced with the non-composite one.

During the experiment, the heat sink temperature of the LD was kept at 30 °C and the pump wavelength was changed from 789.2 to 794.06 nm as the pump power increased from 1 to 66 W, which was detected using a spectrometer (HR4000, Ocean, USA). The LD pump source presented an apparent wavelength drift with increasing the output power, thereby influencing the pump absorption efficiency. Therefore, in this letter, we experimentally measured the pump absorption coefficient of the composite crystal together with the pump wavelength. This measurement was done by recording the transmitted power of pump 1 under non-lasing condition, with the crystal cooled by liquid N$_2$ and the incident power of pump 1 did not exceed 21 W, to avoid thermal fracture of the crystal. The pump-induced increase in temperature within the crystal would significantly influence the measured absorption coefficient[14], therefore, we emphasized that the incident power of pump 1 should not

be attenuated during the measurement to provide a more appropriate depiction of the pump absorption efficiency of the Tm, Ho:YVO$_4$ crystal. Figure 2 shows the measured results wherein the power of pump 1 increased from 1.1 to 20.9 W (corresponding to the total pump power increased from 2.4 to 40.2 W), the pump absorption coefficient increased from 2.45 to about 2.8 cm^{-1}, and the corresponding pump wavelength shifted from 789.32 to 792.55 nm. The inset in Fig. 2 shows the measured absorption coefficient with another LD, with a central wavelength of around 794 nm and an absorption coefficient of about 3.2 cm^{-1}, which are appropriate for the Tm, Ho:YVO$_4$ crystals at high pump power level. This result indicates that more than 90% of the pump power was absorbed by the Tm, Ho:YVO$_4$ crystal.

Considering the pump wavelength red-shifted with increasing pump power, the LD heat sink temperature should be appropriately adjusted to provide the best laser performance because the pump wavelength would also red shift with increasing LD heat sink temperature. For the composite Tm, Ho:YVO$_4$ laser at the highest 66-W pump level, we achieved the most efficient 2-μm CW laser performance when the LD heat sink temperature was set to 30 °C. Although further increases in LD heat sink temperature to higher than 30 °C would lengthen the pump wavelength and result in more efficient pump absorption (Fig. 2), more heat accumulation in the pumped region would diminish laser performance. Similarly, decreasing the LD heat sink temperature to less than 30 °C will shorten the pump wavelength and result in less efficient pump absorption, will also lower the laser performance. Figure 3 shows the laser output power as a function of total incident pump
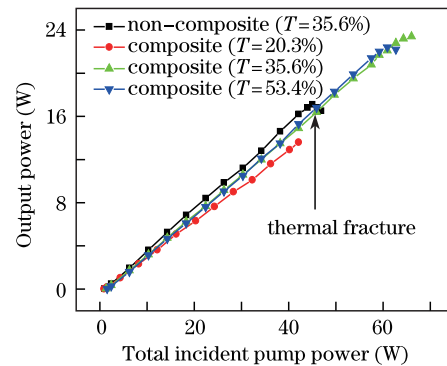
Fig. 3. Output power as a function of the total incident pump power for the composite and non-composite Tm, Ho:YVO$_4$ laser under different output mirror transmissions.
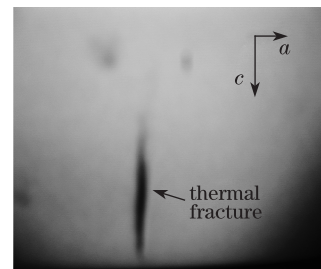
Fig. 4. Thermal fracture of the non-composite Tm, Ho:YVO$_4$ crystal.

power for both the composite and non-composite Tm, Ho:YVO$_4$ lasers (under different output mirror transmissions with the LD heat sink temperature maintained at 30 °C). The best laser performance was achieved using the composite rod, and a stable 23.4-W maximum output power was achieved under a total incident pump power of 66 W ($T = 35.6\%$, output mirror transmission). The corresponding oscillation threshold was about 1.3 W, and the slope efficiency and optical-optical conversion efficiency were 37.3% and 35.4%, respectively. Although the pump wavelength shifted with increasing pump power, the 2-μm laser output power nearly increased linearly in the pump power region and was slightly saturated when the pump power exceeded 60 W. The most likely reason for this saturation is insufficient pump heat removal from the crystal at high pump power. No thermal fractures occurred under the maximum pump power, and the pump can be turned off and on repetitively without power degradation in the experiment. For the non-composite rod (Fig. 3), the oscillation threshold was about 1 W, and had slightly higher slope efficiency ($\sim$39.1%) compared with the composite rod with the same $T = 35.6\%$ output mirror transmission. However, the maximum laser output power of the rod was limited to 17 W under 45-W total incident pump power. When the total incident pump power was larger than 46 W (which corresponds to 25.3 W of power through pump 1 and 20.7 W of power through pump 2), the thermal fracture occurred at the pump 1 end, which had a higher pump power level. A typical micrograph of the non-composite Tm, Ho:YVO$_4$ crystal after thermal fracture is shown in Fig. 4. In the experiment, thermal fracture always occurred along the c-axis, which is attributed to larger the thermal expansion coefficient along c-axis than a-axis of the YVO$_4$ crystal (the thermal expansion coefficient of YVO$_4$ along the c-axis was 7.2×10^{-6} K^{-1} and that along the a-axis was 3.1×10^{-6} K^{-1}, respectively[15]).

The emission wavelength of the composite Tm, Ho:YVO$_4$ laser was measured using a WDG-30 monochromer (300-mm focal length, 300-lines/mm grating blazed at 2 μm). The chopped light from the exit slice of the monochromer was detected using an InGaAs photodetector connected with a lock-in amplifier (SR850, Stanford, USA). Dual-wavelength oscillation was observed when the laser output power was less than 6 W, which was centered at 2.042 and 2.055 μm (Fig. 5), corresponding to the laser transition from energy levels
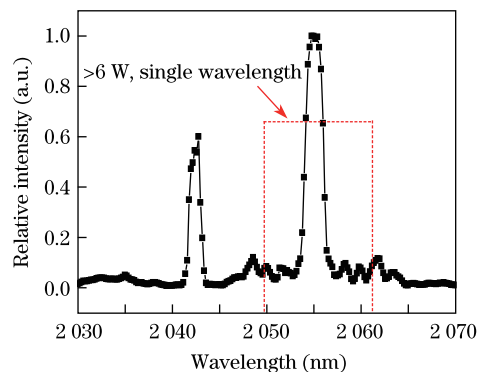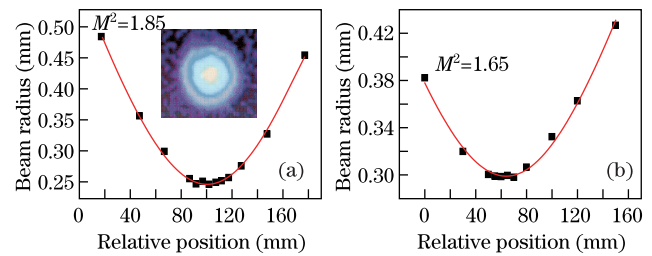
Fig. 6. Brightness determination of the Tm, Ho:YVO$_4$ laser, (a) composite Tm, Ho:YVO$_4$ crystal at 20-W output level, and (b) non-composite Tm, Ho:YVO$_4$ crystal at 14-W output level. Inset in (a), typical two-dimensional beam profiles taken using a Spiricon Pyrocam I pyroelectric camera.

ranging from 5128 to 227 cm^{-1} and from 5128 to 261 cm^{-1}[16]. The 227-cm^{-1} Stark energy level was more severely thermally populated than the 261-cm^{-1} energy level as the pump power increased, which would result in a larger reabsorption loss at the 227-cm^{-1} energy level. Consequently, only the laser transition from 5 128 to 261 cm^{-1} at a lasing wavelength of 2.055 μm, occurred when the output power was larger than 6 W. A similar phenomenon was observed with the lasing wavelength for the non-composite Tm, Ho:YVO$_4$ laser in the experiment.

Figures 6(a) and (b) show the laser beam radii measured via the 90/10 knife-edge technique[17] at 20-W and 14-W output power for composite and non-composite Tm, Ho:YVO $_4$ laser, respectively. The data were fitted using least square analysis of the standard mix-mode Gaussian beam propagation equations to determine the beam quality or M^2 parameter. For the non-composite Tm, Ho:YVO$_4$ laser, the M^2 was determined to be about 1.65, whereas the M^2 was about 1.85 for the composite rod, which indicated that high-brightness 2-μm laser output were obtained from both the non-composite and composite Tm, Ho:YVO$_4$ laser.

In conclusion, an efficient high-power high-brightness 2-μm CW laser with double-end, diffusion-bonded Tm, Ho:YVO$_4$ crystal is demonstrated in this letter. Considering the composite Tm, Ho:YVO$_4$ reduced the thermal stress, a maximum CW output power of 23.4 W is achieved at 2.05 μm, which is about 1.37 times higher than that of the non-composite rod. The corresponding slope efficiency and optical–optical conversion efficiency are 37.3% and 35.4%, respectively. The beam quality M^2 factor is determined to be about 1.85 at 20-W output level with circularly symmetric beam spot.

References

1. B. Yao, Y. Ju, Y. Wang, and W. He, Chin. Opt. Lett. **6**, 68 (2008).
2. E. Lippert, H. Fonnum, G. Arisholm, and K. Stenersen, Opt. Express **18**, 26475 (2010).
3. E. Lippert, G. Rustad, G. Arisholm, and K. Stenersen, Opt. Express **16**, 13878 (2008).
4. H. Peng, K Zhang, L. Zhang, Y Hang, J. Xu, Y. Tang, Y Cheng, J Xiong, C. Zhao, G. Chen, and X. He, Chin. Opt. Lett. **8**, 63 (2010).
5. G. Rustad and K. Stenersen, IEEE J. Quantum Electron. **32**, 1645 (1996).
6. W. He, B. Yao, Y. Ju, and Y. Wang, Opt. Express **14**, 11653 (2006).

Fig. 5. Output spectrum of the composite Tm, Ho:YVO$_4$ laser.

7. B. Yao, G. Li, P. Meng, G. Zhu, Y. Ju, and Y. Wang, Laser Phys. Lett. **7,** 857 (2010).

8. X. Peng, L. Xu, and A. Asundi, IEEE J. Quantum Electron. **38,** 1291 (2002).

9. X. Cheng, J. Xu, Y. Hang, G. Zhao, and S. Zhang, Chin. Opt. Lett. **9,** 091406 (2011).

10. T. Li, Z. Zhuo, X. Li, H. Yang, and Y. Zhang, Chin. Opt. Lett. **5,** 175 (2007).

11. M. Tsunekane, N. Taguchi, T. Kasamatsu, and H. Inaba, IEEE J. Sel. Top. Quantum Electron. **3,** 9 (1997).

12. G. Li, B. Yao, P. Meng, X. Duan, Y. Ju, and Y. Wang, Opt. Mat. **33,** 937 (2011).

13. B. Yao, W. Wang, K. Yu, G. Li, and Y. Wang, Chin. Opt. Lett. **10,** 071402 (2012).

14. B. M. Walsh, G. W. Grew, and N. P. Barnes, J. Phys. Chem. Solids **67,** 1567 (2006).

15. J. C. Bermudez, V. J. Pinto-Robledo, A. V. Kir'yanov, and M. J. Damzen, Opt. Commun. **210,** 75 (2002).

16. S. Gołab, P. Solarz, G. Dominiak-Dzik, T. Lukasiewicz, M. irkowicz, and W. Ryba-Romanowski, Appl. Phys. B **74,** 237 (2002).

17. J. M. Khosrofian and B. A. Garetz, Appl. Opt. **22,** 3406 (1983).